JOURNAL OF COMPUTATIONAL PHYSICS 13, 100–113 (1973)

Numerical Convective Schemes Based on Accurate Computation of Space Derivatives

JENÖ GAZDAG

IBM Corporation, Palo Alto Scientific Center,
2670 Hanover Street, Palo Alto, California 94304

Received February 28, 1972

A numerical procedure is developed for the solution of partial differential equations for the convection of scalar variables. An important feature of this approach is that the space derivatives are computed with very high accuracy by means of Fourier transform methods. By this method a forward marching problem involves discrete time steps but space derivatives are accurate within the limit to which a distribution can be defined on a finite set of meshpoints. Expressions are derived for the amplitude error and phase error, which are verified by computer experiments for the two-dimensional case. This numerical method is applied to the solution of Burgers' equation. The accuracy of the numerical solutions indicates that the method is well suited for the solution of non-linear partial differential equations with other than periodic boundary conditions.

1. INTRODUCTION

Numerical methods for obtaining solutions to initial value problems in "fluid mechanics" and "plasma physics" fall roughly into two categories: (1) transform methods, in which the variables are expressed in terms of orthogonal polynomials; and (2) finite difference methods. The former approach is usually very accurate for problems with simple boundaries [1, 2]. The latter, however, is more versatile and more easily applicable to wide classes of realistic problems [3–5]. Unfortunately, finite difference methods for partial differential equations seldom achieve more than a rather modest accuracy in practice [5, p. 24; 6]. Since the appearance of the work of Roberts and Weiss [7], it has become well understood that the shortcomings of finite difference methods are related to the dispersion and the dissipation present in the numerical approximations. Significant improvement in reduced phase errors with higher order schemes was recognized in their paper [7] although such errors had been discussed previously [8, 9]. Experimental behavior in simple flow situations together with stability analyses were studied by Crowley [10, 11].

The two main sources of error in the solution of initial value problems by finite

difference methods are due to the following: (1) the time derivatives are approximated by truncated Taylor series; and (2) the space derivatives are replaced by some finite difference expression. Space differencing errors can be minimized or even eliminated by the accurate computation of the space derivative terms. A numerical method based on this principle can be expected to possess similar accuracy as the corresponding transform method if similar time differencing methods are employed. Indeed, it was found by Orszag [12] that the pseudospectral (collocation) approximation [13] and the spectral (Galerkin) approximation [1] give similar errors. In the pseudospectral approximation the space derivatives are computed by Fourier methods [13] and "leapfrog" (or midpoint rule) time differencing is used to march forward in time.

In this paper we shall study higher order numerical methods in which the space derivative terms are computed with high accuracy. In our approach to time differencing we start from a Taylor series in t, following in principle Lax and Wendroff [5, p. 302]. The time derivatives are then substituted by expressions containing only space derivative terms. The numerical evaluation of the space derivative terms is based on the use of finite Fourier series. In this respect our method is similar to the pseudospectral approximation [12, 13].

Let $\zeta(\mathbf{x}, t)$ be some distribution with periodic boundary conditions of period 2π in all space variables $\mathbf{x} = (x_1, \ldots, x_j, \ldots, x_n)$. We shall assume that the principal domain is partitioned by a uniform mesh of size $M_1 \times M_2 \cdots \times M_n$ such that the location of the meshpoints is given by

$$x_j = m_j \Delta x_j ; \qquad m_j = 0, 1, 2, \ldots, M_j - 1 \tag{1}$$

where

$$\Delta x_j = 2\pi / M_j \tag{2}$$

for any $j = 1, 2, \ldots, n$. By denoting the collection of all meshpoints as defined above by R, the finite Fourier transform Z of ζ can be written as [14]

$$Z(\mathbf{k}, t) = \frac{1}{M_1 M_2 \cdots M_n} \sum_{\mathbf{x} \in R} \zeta(\mathbf{x}, t) \exp(-i\mathbf{k} \cdot \mathbf{x}) \tag{3}$$

where $i = (-1)^{1/2}$ and $\mathbf{k}$ is the wave vector

$$\mathbf{k} = (k_1, \ldots, k_j, \ldots, k_n) \tag{4}$$

whose components assume integer values within the limits

$$-K_j < k_j \leqslant K_j ; \qquad K_j = M_j/2 \tag{5}$$

where K_j is the wave number of the shortest wave component in the x_j direction (often referred to as the "$2\Delta x$" wave).

From $Z(k, t)$ the partial derivatives of $\zeta(x, t)$ with respect to x_j are computed as

$$\frac{\partial \zeta(\mathbf{x}, t)}{\partial x_j} = \sum_{|k_j|<K_j} ik_j Z(\mathbf{k}, t) \exp(i\mathbf{k} \cdot \mathbf{x}) \tag{6}$$

and

$$\frac{\partial^2 \zeta(\mathbf{x}, t)}{\partial x_j^2} = \sum_{k_j=-K_{j-1}}^{K_j} - k_j^2 Z(\mathbf{k}, t) \exp(i\mathbf{k} \cdot \mathbf{x}). \tag{7}$$

The numerical computation of these expressions can be carried out efficiently by the use of the "fast Fourier Transform" (FFT) algorithm [14]. This method of computing the space derivatives gives results that are substantially more accurate than those obtained from finite difference expressions. Owing to this property, numerical methods studied in this paper will be referred to as "accurate space derivative" (ASD) methods.

In Section 2 we shall describe the application of the ASD method to the convective equation. In Section 3 we present a thorough analysis of the amplitude and phase errors for various orders of approximation. These results are valid for the general n-dimensional case. In Section 4 we study the accuracy of the ASD method by means of numerical experiments involving the uniform rotation of a Gaussian distribution. In Section 5 we apply the ASD method to the numerical solution of Burgers' equation, in order to illustrate its accuracy and power in problems involving nonlinear partial differential equations with nonperiodic boundary conditions. The computed Burgers' shock waves are in very good agreement with the exact profiles for a wide range of values of the dissipative parameter.

2. ASD Method for the Convective Equation

In this Section, we develop numerical methods for the n-dimensional convective equation

$$(\partial \zeta / \partial t) + \mathbf{v} \cdot \nabla \zeta = 0 \tag{8}$$

where $\zeta = \zeta(\mathbf{x}, t)$, and $\mathbf{v} = \mathbf{v}(\mathbf{x}, t)$, and furthermore, $\mathbf{v} = (v_1, v_2, \ldots, v_n)$, $\mathbf{x} = (x_1, x_2, \ldots, x_n)$ and ∇ is the n-dimensional *del operator*. For simplicity $\mathbf{v}$ is assumed to be known, although, in general, it is computed at each time step, e.g., by solving the Poisson equation [9, 6].

Suppose that an approximate solution is sought to the initial value problem represented by Eq. (8). The variable ζ is approximated at time $(m + 1)\,\Delta t$ on the

basis of the known values of ζ and $\mathbf{v}$ at time $m\,\Delta t$. This can be done conveniently by expressing $[\zeta[\mathbf{x}, (m+1)\,\Delta t]$ in a truncated Taylor series

$$\zeta^{m+1} = \zeta^m + \frac{\partial \zeta^m}{\partial t}\,\Delta t + \frac{\partial^2 \zeta^m}{\partial t^2}\,\frac{\Delta t^2}{2!} + \cdots + \frac{\partial^p \zeta^m}{\partial t^p}\,\frac{\Delta t^p}{p!} \tag{9}$$

where ζ^m stands for $\zeta(\mathbf{x}, m\,\Delta t)$. The time derivatives of ζ are expressed in terms of the space derivatives of ζ and $\mathbf{v}$ by making use of Eq. (8). By successive differentiation, starting with Eq. (8), we obtain

$$\frac{\partial \zeta}{\partial t} = -\mathbf{v} \cdot \nabla \zeta, \tag{10}$$

$$\frac{\partial^2 \zeta}{\partial t^2} = -\frac{\partial \mathbf{v}}{\partial t} \cdot \nabla \zeta - \mathbf{v} \cdot \nabla \left(\frac{\partial \zeta}{\partial t}\right) \tag{11}$$

$$\vdots \qquad\qquad \vdots$$

$$\frac{\partial^{l+1} \zeta}{\partial t^{l+1}} = -\sum_{i=0}^{l} \frac{l!}{(l-i)!\,i!}\,\frac{\partial^i \mathbf{v}}{\partial t^i} \cdot \nabla \left(\frac{\partial^{l-i} \zeta}{\partial t^{l-i}}\right). \tag{12}$$

For convenience, the superscript m has been omitted in the above equations. All the known variables $\mathbf{v}$ and ζ are given at $t = m\,\Delta t$, hence there is no ambiguity if m is dropped.

It is seen from Eqs. (10–12) that any time derivative of ζ can be obtained from lower order time derivatives of $\mathbf{v}$ and ζ. The substitution of the left-hand side of Eqs. (10–12) in Eq. (9) completes the computation process. The space derivatives in Eqs. (10–12) are computed by the Fourier method as shown in Eqs. (3–6).

3. Analysis of Stability and Accuracy

The prime requirement of a numerical scheme is that it be stable. In the linear stability analysis [6] of convective schemes we study solutions of Eq. (8) for a uniform, constant velocity field, i.e., $\mathbf{v}$ = constant. We shall call the convective scheme stable if all its Fourier components remain bounded and unstable if at least one component is unbounded. The trivial solution of Eq. (8) is

$$\zeta(\mathbf{x}, t) = \exp[i\mathbf{k} \cdot (\mathbf{x} - \mathbf{v}t)] \tag{13}$$

so that the initial configuration

$$\zeta(\mathbf{x}, t) = \exp[i\mathbf{k} \cdot \mathbf{x}] \tag{14}$$

is merely translated by the amount vt in time t, and the solution after a time interval Δt has a phase angle

$$\phi = -\mathbf{k} \cdot \mathbf{v}\, \Delta t. \tag{15}$$

There is no amplitude damping or growth.

Let us consider now the convection of initial configurations given in Eq. (14) by the ASD scheme. Substituting Eqs. (14) and (15) into Eqs. (10–12), and by making use of Eq. (9), assuming that $m = 0$, we obtain

$$\zeta^1 = [1 + i\phi - \phi^2/2! + \cdots + (i\phi)^p/p!]\, \zeta^0. \tag{16}$$

We shall denote the multiplier of ζ^0 in Eq. (16) by λ_p, i.e.,

$$\lambda_p(\phi) = \sum_{l=0}^{p} \frac{(i\phi)^l}{l!}, \tag{17}$$

which we shall refer to as the amplification factor [7]. The subscript p signifies the highest order term in Eqs. (9) and (16). We define the amplitude error in the ASD scheme of order p as

$$\epsilon_p(\phi) = |\lambda_p(\phi)| - 1. \tag{18}$$

The amplitude errors computed numerically from Eqs. (17) and (18) are shown in Fig. 1. The nine curves correspond to different values of p, as indicated. The con-

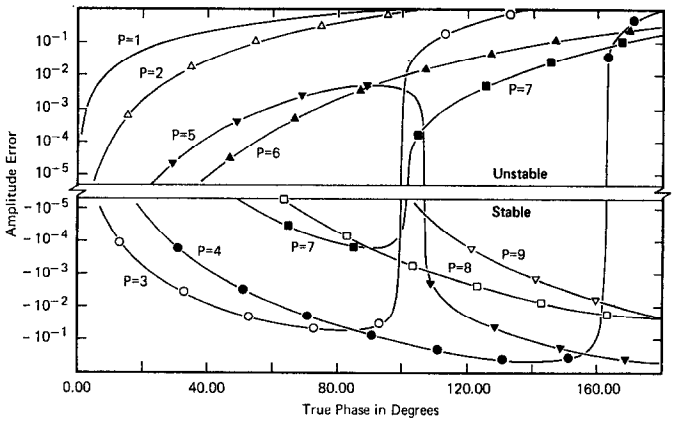

FIG. 1. Amplitude errors ϵ_p as defined by Eq. (18). The true phase is ϕ as per Eq. (15) and p indicates the order of the approximation.

dition for stability for all ϕ values within some range, say

$$-\Phi_p \leqslant \phi \leqslant \Phi_p$$

is that $| \lambda_p | \leqslant 1$, or equivalently that $\epsilon_p \leqslant 0$. This stability condition is satisfied by the ASD schemes whose order is 3, 4, 7, and 8.

In addition to amplitude errors, numerical convective schemes introduce errors in phase causing numerical dispersion. In our analysis of the phase errors we compare the correct phase ϕ, Eq. (15), with the actual phase angle resulting from the numerical convective methods, which for the ASD scheme of order p can be expressed as

$$\phi_p = \cos^{-1}[\mathrm{Re}(\lambda_p)/| \lambda_p |] \tag{19}$$

in which $\mathrm{Re}(\lambda_p)$ is the real part of the amplification factor. In order to express the magnitude of the error relative to the correct phase angle, we define the relative phase error δ_p, for the ASD scheme of order p, as

$$\delta_p = (\phi_p - \phi)/\phi. \tag{20}$$

By making use of Eqs. (17) and (20) δ_p can be determined for any given p and ϕ. The computed results for δ_p are shown in Fig. 2.

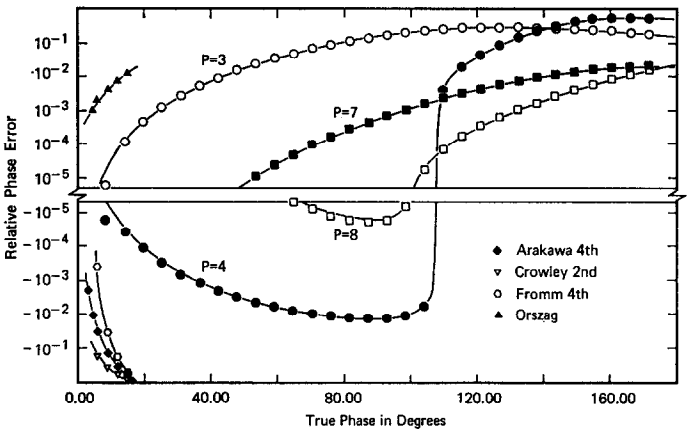

FIG. 2. Comparison of phase errors δ_p. The solid curves ($p = 3, 4, 7$, and 8) were computed from Eq. (20). The superimposed symbols (circle and square) designate computer experimental results. The three sets of results shown in the lower left corner correspond to those of Arakawa (fourth order [1]), Crowley (second order [10]), and Fromm (fourth order [6]). The five symbols in the upper left represent the results of the Galerkin approximation [1].

4. Numerical Experiments: Passive Convection

In order to verify the expressions for the amplitude error (18) and phase error (20) and to test the method we programmed the ASD scheme for the two-dimensional case ($n = 2$). In the first set of numerical experiments the velocity field was chosen as

$$\mathbf{v} = (v_1, v_2) = (1, 1) \tag{21}$$

whose effect is a translation of the initial distribution along the diagonal of the mesh. The initial distribution $\zeta(\mathbf{x}, 0)$ was a delta function to ensure that all Fourier components are present. At one time step Δt later we evaluated the actual amplitude errors and phase errors from the Fourier coefficients of $\zeta(\mathbf{x}, \Delta t)$. We found that the resulting truncation errors agreed remarkably well with those obtained from Eqs. (17) and (20). The phase errors obtained from the numerical experiments are indicated by symbols in Fig. 2.

The second set of computer experiments to test the accuracy of the method was a two-dimensional convection of a passive scalar by a uniform rotation about the center of the mesh with an angular velocity Ω. This problem is regarded as an effective test of the accuracy of numerical convective methods [1, 11, 15, 16]. The initial distribution was specified over a 32×32 mesh as a Gaussian

$$\zeta(\mathbf{x}, 0) = \exp\left\{-\frac{1}{2}\left[\left(\frac{x_1 - x_0}{a}\right)^2 + \left(\frac{x_2}{b}\right)^2\right]\right\} \tag{22}$$

where $x_0 = 8\,\Delta x_1$, $a = 1.41\,\Delta x_1$ and $b = 2\,\Delta x_2$, expressed in multiples of the mesh spacings. The perspective view of the Gaussian distribution is shown in Fig. 3.

The distribution was subjected to a complete revolution (2π) clockwise, followed by one (2π) counterclockwise rotation by reversing the velocity field. The time steps (Δt) were chosen so that a 2π rotation requires exactly 400 time steps. Thus, the Gaussian was expected to be centered over a meshpoint, within some numerical

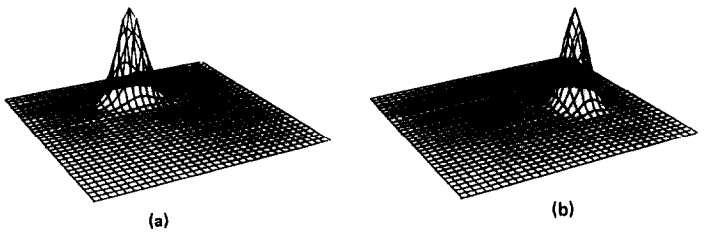

Fig. 3. Perspective view of the Gaussian distribution in Experiment 1 of Table I. (a) At $\pi/2$, (b) At π turn from its initial position. The mesh size is 32×32.

errors, after $\pi/2$, π, $3\pi/2$, and 2π rotations. We were particularly interested in the maximum and minimum values at the mesh point after multiples of quarter revolutions. These results are shown in Table I.

TABLE I
Uniform Rotations of the Gaussian Distribution

Experiment	Order of scheme p	Rotations		ϕ_{max} in degrees (approx.)	$\frac{2\pi}{\Omega\Delta t}$	Maximum at a meshpoint	Minimum at a meshpoint
		Clockwise	Counter Clockwise				
		0	0			1.0000	0.0000
		$\pi/2$	0			0.9996	0.0000
		π	0			0.9991	0.0000
1	3	$3\pi/2$	0	80	400	0.9987	0.0000
		2π	0			0.9982	0.0000
		2π	π			0.9973	0.0000
		2π	2π			0.9964	0.0000
		0	0			1.0000	0.0000
		$\pi/2$	0			0.9997	0.0000
		π	0			0.9995	0.0000
2	4	$3\pi/2$	0	80	400	0.9992	0.0000
		2π	0			0.9989	0.0000
		2π	π			0.9984	0.0000
		2π	2π			0.9979	0.0000

5. Numerical Methods for Burgers' Equation

Burger's equation reads

$$(\partial u/\partial t) + u(\partial u/\partial x) = \nu(\partial^2 u/\partial x^2) \tag{23}$$

where ν is the coefficient of diffusivity [17], also known as the dissipative parameter [18]. Equation (23) approximates the motion of a plane wave of small but finite amplitude. For the initial wave form

$$u(x, 0) = \begin{cases} u_1, & x \leqslant 0 \\ 0, & x > 0 \end{cases}$$

Equation (23) has a steady solution of the form [18]

$$u = (1/2)\, u_1[1 - \tanh(u_1\zeta/4\nu)] \tag{25}$$

where $\zeta = x - \lambda t$, $\lambda = \text{const} = u_1/2$.

We studied two different numerical methods based on the ASD principle for solving Burgers' equation. In the first method the solution is advanced by computing the contributions from the nonlinear convective term and the dissipative term separately in each time step. In the second method, which is considerably more accurate than the first, we advance the solution by accounting for both the convective and diffusive terms simultaneously.

In order to satisfy the conditions expressed in Eq. (24) the principle domain

$$D = \{x; 0 \leqslant x \leqslant L\} \tag{26}$$

is partitioned into two subdomains

$$D = D_0 + D_1$$

as shown in Fig. 4. Here D_1 is the time computational domain over which new u values are computed. The values of u over D_0 are fixed and are being kept constant throughout the entire computation. The unique purpose of D_0 is to provide a smooth transition between the two end points of D_1 and to assure periodicity over D. This configuration permits the computation of the space derivatives of u by the Fourier method outlined earlier. In the numerical examples considered here the length of D_0 was set equal to 0.6 over which $u(x, t)$ was given by

$$u(x, t) = \begin{cases} 0; & 0 \leqslant x < 0.1 \\ 0.5[1 - \cos((x - 0.1)\,\pi/0.3)]; & 0.1 \leqslant x < 0.4 \\ 1; & 0.4 \leqslant x < 0.6 \end{cases} \tag{27}$$

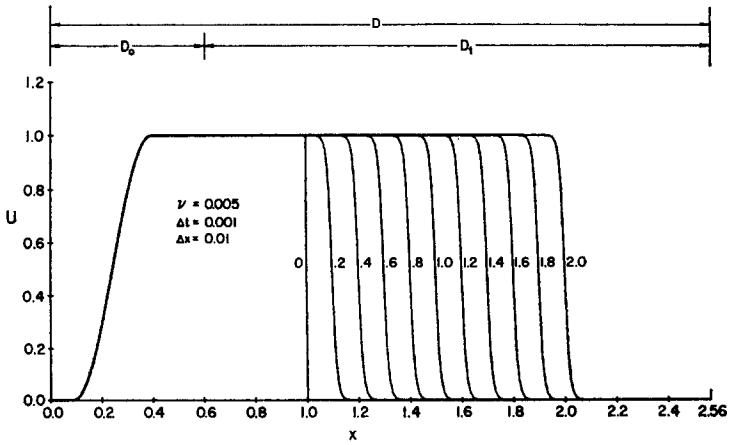

FIG. 4. Evolution of the numerical solution (method B) of Burgers' equation from an initial condition in the form of a step function, $\nu = 0.005$. The time separation between any two successive plots is 0.2 time units; the numbers on the curves are values of time.

as shown in Fig. 4. In what follows we describe these two numerical approaches to the solution of Burgers' equation.

Method A

The essence of this solution method is to alternate between the following two steps: (1) compute an intermediate solution

$$\tilde{u}(t + \Delta t) = u(t) + \frac{\partial u(t)}{\partial t}\Delta t + \frac{\partial^2 u(t)}{\partial t^2}\frac{\Delta t^2}{2} + \frac{\partial^3 u(t)}{\partial t^3}\frac{\Delta t^3}{3!} \tag{28}$$

where

$$\frac{\partial u}{\partial t} = -u\frac{\partial u}{\partial x}, \tag{29}$$

$$\frac{\partial^2 u}{\partial t^2} = -\frac{\partial u}{\partial t}\frac{\partial u}{\partial x} - u\frac{\partial}{\partial x}\left(\frac{\partial u}{\partial t}\right), \tag{30}$$

$$\frac{\partial^3 u}{\partial t^3} = -\frac{\partial^2 u}{\partial t^2}\frac{\partial u}{\partial x} - 2\frac{\partial u}{\partial t}\frac{\partial}{\partial x}\left(\frac{\partial u}{\partial t}\right) - u\frac{\partial}{\partial x}\left(\frac{\partial^2 u}{\partial t^2}\right), \tag{31}$$

by using only the convective term; (2) advance the solution using only the diffusion term by means of the finite Fourier transform method [19]

$$u(t + \Delta t) = F^{-1}[\exp(-\nu k^2 \Delta t) F(\tilde{u})] \tag{32}$$

where the Fourier transform operation and its inverse are denoted by F and F^{-1} respectively, and k is the wave number.

Method B

In this solution method we compute $u(t + \Delta t)$ from $u(t)$ by the following expression:

$$u(t + \Delta t) = u(t) + \frac{\partial u(t)}{\partial t}\Delta t + \frac{\partial^2 u(t)}{\partial t^2}\frac{\Delta t^2}{2} + \frac{\partial^3 u(t)}{\partial t^3}\frac{\Delta t^3}{3!}. \tag{33}$$

The time derivatives in Eq. (33) are computed from Eq. (23) by successive differentiation as follows:

$$\frac{\partial u}{\partial t} = -u\frac{\partial u}{\partial x} + \nu\frac{\partial^2 u}{\partial x^2}, \tag{34}$$

$$\frac{\partial^2 u}{\partial t^2} = -\frac{\partial u}{\partial t}\frac{\partial u}{\partial x} - u\frac{\partial}{\partial x}\left(\frac{\partial u}{\partial t}\right) + \nu\frac{\partial^2}{\partial x^2}\left(\frac{\partial u}{\partial t}\right), \tag{35}$$

$$\frac{\partial^3 u}{\partial t^3} = -\frac{\partial^2 u}{\partial t^2}\frac{\partial u}{\partial x} - 2\frac{\partial u}{\partial t}\frac{\partial}{\partial x}\left(\frac{\partial u}{\partial t}\right) - u\frac{\partial}{\partial x}\left(\frac{\partial^2 u}{\partial t^2}\right) + \nu\frac{\partial^2}{\partial x^2}\left(\frac{\partial^2 u}{\partial t^2}\right). \tag{36}$$

The x derivative terms in Eqs. (29–31) and (34–36) are computed by Fourier methods over the principal domain D, however, the solutions, Eqs. (28), (32), and (33), are advanced only over D_1 (Fig. 4).

All numerical computations of Burgers' equation were performed with $\Delta t = 0.001$ and $\Delta x = 0.01$ using 256 meshpoints to represent D. From the initial condition (24) the travelling wave profile (Fig. 4) evolves into what approximates the exact analytic result (25). Computed values of these profiles at the meshpoints, together with the exact values (25) are given in Tables II and III, at $t = 0.85$, for methods A and B, respectively.

These tables indicate similar accuracy for both methods in the $\nu = 0.002$ case. For greater ν values, however, method B is clearly superior. The remarkable accuracy of method B is demonstrated by the $\nu = 0.01$ case in which the error is of the order of 0.01 % of the maximum value u_1, and the velocity of the wave profile is 0.4999, i.e., slightly lower than the theoretical velocity of propagation which is 0.5.

In comparing these solution methods the greater accuracy of B is attributed to its small truncation errors $O(\Delta t^4)$. In method A the contributions due to the convective and diffusive terms are computed independently with similar (or better) accuracy than in B. The simple addition of the contributions from the two competing terms, however, results in truncation errors $O(\Delta t^2)$, i.e., method A is only

TABLE II

Comparison of Analytic with Numerical Results from Method A for the wave in Burgers' Equation (The wave profile amplitude $u(x)$ is given as a function of distance.)

$u(x)$

	$\nu = 0.002$		$\nu = 0.005$		$\nu = 0.01$	
x	Exact	Computed	Exact	Computed	Exact	Computed
1.37	1.000	0.992	0.997	0.996	0.952	0.950
1.38	1.000	1.003	0.993	0.991	0.923	0.920
1.39	1.000	0.990	0.981	0.979	0.879	0.876
1.40	0.999	1.005	0.951	0.948	0.815	0.812
1.41	0.991	0.978	0.876	0.872	0.727	0.725
1.42	0.901	0.910	0.723	0.719	0.618	0.616
1.43	0.429	0.429	0.489	0.489	0.495	0.495
1.44	0.058	0.066	0.261	0.264	0.373	0.374
1.45	0.005	0.007	0.115	0.118	0.265	0.267
1.46	0.000	0.001	0.046	0.048	0.179	0.181
1.47	0.000	0.001	0.017	0.018	0.117	0.119
1.48	0.000	0.000	0.006	0.007	0.074	0.076
1.49	0.000	0.000	0.002	0.003	0.047	0.048

TABLE III

Comparison of Analytic with Numerical Results from Method B for the Wave in Burgers' Eq. (The wave profile amplitude $u(x)$ is given as a function of distance.)

$u(x)$

	$\nu = 0.002$		$\nu = 0.005$		$\nu = 0.01$	
x	Exact	Computed	Exact	Computed	Exact	Computed
1.37	1.000	0.993	0.9975	0.9972	0.9524	0.9524
1.38	1.000	1.005	0.9932	0.9930	0.9239	0.9239
1.39	1.000	0.991	0.9818	0.9814	0.8805	0.8805
1.40	0.999	1.007	0.9520	0.9517	0.8171	0.8172
1.41	0.991	0.979	0.8795	0.8792	0.7305	0.7305
1.42	0.901	0.919	0.7286	0.7285	0.6218	0.6218
1.43	0.428	0.428	0.4969	0.4969	0.4993	0.4993
1.44	0.058	0.062	0.2666	0.2667	0.3769	0.3768
1.45	0.005	0.005	0.1179	0.1180	0.2684	0.2683
1.46	0.000	0.000	0.0469	0.0469	0.1820	0.1819
1.47	0.000	0.000	0.0178	0.0178	0.1189	0.1189
1.48	0.000	0.000	0.0066	0.0066	0.0757	0.0756
1.49	0.000	0.000	0.0024	0.0024	0.0473	0.0472

a first order method. According to our analysis the considerably smaller accuracy for the $\nu = 0.002$ example in both methods A and B is not the consequence of the inaccuracy of the numerical schemes but is the result of the truncation of the spectrum in k space. More accurate representation of such steep profile requires higher wave numbers than those that can be supported by the computational mesh used.

6. Concluding Remarks

Numerical ASD methods own their accuracy to the almost exact computation of the space derivative terms. These operations, Eqs. (1–7), require more computer time than the approximation of the derivatives by simple finite difference expressions in almost all 1-dimensional problems. The two-dimensional scalar convection simulations using the third-order scheme (Experiment 1 in Table I) required about 0.09 sec per time step. These calculations were performed on an IBM System/360 Model 195 computer. We have no accurate timing information available for finite difference methods. As an order-of-magnitude comparison, the computer time requirements of the fourth-order ASD method were estimated [20] to be about two times that of the fourth-order finite difference scheme of Fromm [3].

In the case of three-dimensional problems, however, the ASD schemes ($p = 3$ or 4) are expected to be faster than Fromm's fourth-order finite difference method. All programs were written in the FORTRAN language. The speed of computations for the ASD scheme could be improved by at least a factor of two if an assembler-language-written fast Fourier transform routine is used.

We have derived the expressions for the phase error and amplitude error for the ASD convective schemes. These results were verified by computer experiments. There is a remarkably good agreement between *the theoretical and the numerical results*. Both phase and amplitude error can be expressed in terms of a single variable ϕ. This variable is the theoretical change in phase angle (in one time step) of the Fourier component of the scalar variable convected by a uniform velocity field. This "true phase" ϕ is defined by Eq. (15) for the general n-dimensional case. Therefore, our results regarding amplitude and phase error are independent of dimensionality.

As a nonlinear example to test the feasibility and accuracy of the ASD methods we studied the numerical solutions of Burgers' equation (23). We have demonstrated that the ASD convective scheme is well suited to the numerical solution of nonlinear problems. The results of Table III demonstrate that the ASD method (B) can be applied to partial differential equations which are more general than the convective equation. On the basis of the experience gained from solving Burgers' equation with conditions specified by Eq. (24), we can conclude that the ASD methods are applicable to problems with other than periodic boundary conditions.

ACKNOWLEDGMENTS

I wish to express my gratitude to J. E. Fromm for the many stimulating discussions and his valuable suggestions. His earnest interest in this work, which he demonstrated by testing the ASD method in real flow simulations, was a source of encouragement. I wish to express my thanks to B. H. Armstrong, J. Canosa, H. P. Flatt, H. G. Kolsky, and Professor O. Buneman for their interest and the discussion of several aspects of the ASD method.

REFERENCES

1. S. A. ORSZAG, *J. Fluid Mech.* **49** (1971), 75.
2. T. P. ARMSTRONG, R. C. HARDING, G. KNORR, AND D. MONTGOMERY, Solution of Vlasov's Equation by Transform Methods, *in* "Methods in Computational Physics," Vol. 9, pp. 30–84, Academic Press, New York, 1970.
3. J. E. FROMM, *IBM J. Res. Dev.* **15** (1971), 186.
4. JOSÉ CANOSA, JENÖ GAZDAG, J. E. FROMM, AND B. H. ARMSTRONG, *Phys. Fluids* **15** (1972), 2299.
5. R. D. RICHTMEYER AND K. W. MORTON, "Difference Methods for Initial-Value Problems," Interscience Publishers, Second ed., 1967.

6. J. E. FROMM, *Phys. Fluids (Suppl. 2)* **12** (1969), 3.
7. K. V. ROBERTS AND N. O. WEISS, *Math. Comp.* **20** (1966), 272.
8. C. E. LEITH, Numerical Simulation of the Earth's Atmosphere, *in* "Methods in Computational Physics," Vol. 4, pp. 1–28, Academic Press, New York, 1965.
9. A. ARAKAWA, *J. Comp. Phys.* **1** (1966), 119.
10. W. P. CROWLEY, *J. Comp. Phys.* **1** (1967), 471.
11. W. P. CROWLEY, *Mon. Weath. Rev.* **96** (1968), 1.
12. S. A. ORSZAG, *Stud. in Appl. Math.* **51** (1972), 253.
13. S. A. ORSZAG, *Stud. in Appl. Math.* **50** (1971), 293.
14. J. W. COOLEY, P. A. W. LEWIS, AND P. D. WELCH, "The Finite Fourier Transform," *IEEE Tran.* AU-17, 77–85 (1969).
15. C. R. MOLENKAMP, *J. Appl. Meteor.* **7** (1968), 160.
16. S. Z. BURSTEIN AND A. A. MIRIN, *J. Comp. Phys.* **5** (1970), 547.
17. T. D. TAYLOR, E. NDEFO, AND B. S. MASON, *J. Comp. Phys.* **9** (1971), 99.
18. A. JEFFREY AND T. KAKUTANI, *SIAM Review* **14** (1972), 582.
19. J. GAZDAG AND J. CANOSA, "Numerical Solution of Fisher's Equation," Report No. 320-3309, IBM Scientific Center, Palo Alto, California, November 1972.
20. J. E. FROMM, private communications.